On the Hadronuclear Origin of the TeV Emission of Ap Librae

Zhao-Hua Xie[1], Lei-Ming Du[1*], Yun-Bing Xu[1], Rui Xue[2*], and Ze-Rui Wang[3*]

[1]*Department of Physics, Yunnan Normal University, Kunming 650500, China*
[2]*Department of Physics, Zhejiang Normal University, Jinhua 321004, China*
[3]*College of Physics and Electronic Engineering, Qilu Normal University, Jinan 250200, China*

(Received 19 October 2025; accepted manuscript online 12 December 2025)

We investigate the origin of the very-high-energy (VHE; $\geqslant$100 GeV) γ-ray emission from the low-synchrotron-peaked BL Lac object Ap Librae within the framework of a one-zone hadronuclear (pp) interaction model. Conventional leptonic and hadronic scenarios (including photohadronic processes and proton synchrotron emission) have encountered difficulties in reproducing the unusually broad GeV–TeV spectrum of this source without invoking extreme physical conditions. In this work, we construct a one-zone pp model that incorporates both leptonic and hadronuclear components and apply it to fit the multiwavelength spectral energy distribution of Ap Librae. Our results show that the optical-GeV emission can be well explained by leptonic emission from primary electrons, while the TeV emission is naturally accounted for by γ-rays from neutral pion decay in pp interactions. The required total jet power is found to be $\sim 1.8 \times 10^{46}\,\mathrm{erg\cdot s^{-1}}$, which corresponds to half of the Eddington luminosity of the central supermassive black hole. Compared with previous hadronic models that demand super-Eddington energetics, our approach provides a more physically reasonable explanation for the VHE spectrum of Ap Librae.

DOI: 10.1088/0256-307X/43/2/021101 CSTR: 32039.14.0256-307X.43.2.021101

1. Introduction. Blazars represent the most extreme subclass of active galactic nuclei (AGNs), characterized by relativistic jets that are closely aligned with the observer's line of sight.[1,2] The multi-wavelength spectral energy distribution (SED) is dominated by non-thermal jet emission and typically exhibits a double-hump structure. The low-energy hump, spanning from radio to UV/X-ray bands, is generally attributed to synchrotron radiation from accelerated relativistic electrons. In contrast, the origin of the high-energy hump, extending from X-rays to γ-ray, is interpreted by leptonic models and/or hadronic models. In leptonic models, the high-energy hump is explained by inverse Compton (IC) radiation from relativistic electrons that up-scatter soft photons emitted by the same electron population (synchrotron-self Compton, SSC; Refs. [3–5]), or soft photons originated from external photon fields (external Compton, EC; Ref. [6]). Hadronic models, on the other hand, attribute the high-energy hump to proton synchrotron radiation as well as to secondary particles generated in hadronic interactions (including photohadronic and hadronuclear interactions), and internal $\gamma\gamma$ pair production account for the high-energy bump.[7–21]

Ap Librae is a nearby low-synchrotron-peaked BL Lac object (LBL; $z \approx 0.049$) and one of the very few members of its class detected at very high energies (VHEs; $\geqslant$100 GeV).[22] Unlike the majority of VHE-detected blazars, which are typically high-synchrotron-peaked BL Lacs (HBLs), Ap Librae displays an unusually broad high-energy component extending from X-rays to multi-TeV γ-rays, spanning nearly nine orders of magnitude in frequency.[23,24] This extreme spectral shape, together with the detection of a kiloparsec-scale X-ray jet,[25] makes Ap Librae an exceptional and challenging source for theoretical interpretation. Conventional one-zone SSC models, which successfully describe many HBLs, fail to reproduce the broad GeV–TeV emission of Ap Librae.[24,26] Even when EC components are included, the models often underestimate either the X-ray or the γ-ray fluxes, highlighting an intrinsic difficulty in explaining the source within standard leptonic frameworks.[27,28] To address these challenges, several alternative scenarios have been proposed. One possibility is that the VHE emission originates not in the compact blazar core but in the extended kpc jet, where relativistic electrons upscatter cosmic microwave background (CMB) photons (the IC/CMB model[24,28]). More recently, reference [29] highlighted the role of circumnuclear dust, showing that IC scattering of both CMB and dust photons by electrons in the core and sub-kpc jet can naturally reproduce the unusually broad high-energy component. On the other hand, reference [27] introduced a "blob-in-jet" framework, where interactions between a compact blob, the parsec-scale jet, and external photon fields can account for both the GeV–TeV spectrum, albeit with increased model complexity. Beyond purely leptonic models, hadronic processes have also been considered. Reference [30] explored a proton synchrotron origin of the X-ray and γ-ray emissions in the extended jet,

*Corresponding authors. Email: duleiming@ynnu.edu.cn; ruixue@zjnu.edu.cn; zerui_wang62@163.com
© 2026 Chinese Physical Society and IOP Publishing Ltd. All rights, including for text and data mining, AI training, and similar technologies, are reserved.

finding that it could explain the data but only under extreme conditions, such as ultra-high proton energies and super-Eddington jet powers. Reference [12] instead proposed a lepto-hadronic scenario in which photohadronic interactions in the compact region contribute significantly to the TeV band, though again at the cost of very high jet energetics.

Building on these developments, recent works have highlighted that hadronuclear (pp) interactions in relativistic jets may provide an alternative channel for producing TeV γ-ray in blazars.[16,18–21,31–35] These studies suggest that π^0 decay γ-rays generated in pp interactions can, under certain conditions, reproduce the observed VHE spectra and even account for hard TeV components, offering a viable complement to conventional leptonic, proton synchrotron and photohadronic models. However, a persistent challenge is that many hadronic scenarios tend to require extreme assumptions, such as ultra-high proton energies or jet powers far exceeding the Eddington luminosity of the central super-massive black hole (SMBH). In this work, we make a first attempt to interpret the multiwavelength SED of Ap Librae using pp-induced emission, demonstrating that such modeling can be carried out under sub-Eddington jet powers and physically reasonable parameters in a one-zone framework. In Section 2, we present the model description. In Section 3, we employ the one-zone pp model to fit the multiwavelength SED of Ap Librae. Discussion and conclusion are given in Section 4. Throughout the paper, the cosmological parameters $H_0 = 69.6\,\mathrm{km{\cdot}s^{-1}{\cdot}Mpc^{-1}}$, $\Omega_0 = 0.29$, and $\Omega_\Lambda = 0.71$[36] are adopted.

2. Model Description.

Building on the conventional one-zone leptonic framework, we further incorporate hadronic emission from pp interactions, where the cold protons originate within the jet. The exact jet composition remains uncertain, with both pure electron–proton plasma and pure electron–positron plasma scenarios having been extensively investigated.[37–41] In our modeling, we do not specify the jet composition explicitly; instead, we assume that the total jet power is primarily carried by relativistic and cold protons,[33] with the cold component representing those protons that are not accelerated within the jet. In the one-zone modeling of blazars' emission, it is widely assumed that all the non-thermal radiation of the jet comes from a compact spherical emitting region. It is composed of a plasma of charged particles in a uniformly magnetic field B with radius R and moving with bulk Lorentz factor $\Gamma = (1-\beta_\Gamma^2)^{-1/2}$, where $\beta_\Gamma c$ is the jet speed along the jet, at a viewing angle $\theta_{\rm obs}$ with respect to the observers' line of sight. Due to the beaming effect, the observed radiation is strongly boosted by a relativistic Doppler factor $\delta_{\rm D} = [\Gamma(1-\beta_\Gamma\cos\theta_{\rm obs})]^{-1}$. In this work, by assuming $\theta_{\rm obs} \lesssim 1/\Gamma$ for blazars, we have $\delta_{\rm D} \approx 2\Gamma$. In this section, the parameters with superscript "obs" are measured in the observers' frame, those with superscript "AGN" are measured in the AGN frame, whereas the parameters without the superscript are measured in the comoving frame, unless specified otherwise.[42]

2.1. Leptonic Emission.

In our modeling, we assume that primary relativistic electrons are injected at a constant rate following a smooth broken power-law energy distribution,[43] described by $\dot{Q}_{\rm e}^{\rm inj}(\gamma_{\rm e}) = \dot{Q}_{\rm e,0}\gamma_{\rm e}^{-p_{\rm e,1}}[1+(\gamma_{\rm e}/\gamma_{\rm e,b})^{(p_{\rm e,2}-p_{\rm e,1})}]^{-1}H(\gamma_{\rm e};\gamma_{\rm e,min},\gamma_{\rm e,max})$, where $H(x;x_1,x_2)$ is defined for $x_1 \le x \le x_2$, $\gamma_{\rm e,min/b/max}$ represent the minimum, break, and maximum Lorentz factors, and $p_{\rm e,1/2}$ represent the spectral indices before and after $\gamma_{\rm e,b}$. Given an electron injection luminosity $L_{\rm e,inj}$, $\dot{Q}_{\rm e,0}$ can be determined by $\int \gamma_{\rm e} m_{\rm e}c^2 \dot{Q}_{\rm e}^{\rm inj}(\gamma_{\rm e})\mathrm{d}\gamma_{\rm e} = 3L_{\rm e,inj}/4\pi R^3$, where $m_{\rm e}$ is the electron rest mass. When the injection process is balanced by radiative cooling and/or particle escape, a steady-state electron energy distribution is established, which can be approximated as $N_{\rm e}(\gamma_{\rm e}) \approx \dot{Q}_{\rm e}^{\rm inj}(\gamma_{\rm e})\min\{t_{\rm cool}, t_{\rm dyn}\}$, where $t_{\rm dyn} = R/c$ is the dynamical timescale of the blob, and $t_{\rm cool} = \frac{3m_{\rm e}c}{4\gamma_{\rm e}\sigma_{\rm T}(U_{\rm B}+\kappa_{\rm KN}U_{\rm soft})}$ is the radiative cooling timescale, where $\sigma_{\rm T}$ is the Thomson scattering cross section, $\kappa_{\rm KN}$ is a numerical factor accounting for the Klein–Nishina effect,[44] $U_{\rm B} = B^2/8\pi$ is the energy density of the magnetic field, and $U_{\rm soft}$ is the energy density of target photons, including synchrotron photons and photons from external fields. As suggested by Ref. [45], LBLs may represent masquerading BL Lacs, in which external photons play a significant role in IC scattering. Consequently, in addition to synchrotron photons, we also include external photon fields from the broad-line region (BLR) and the dusty torus (DT). To evaluate their contributions, we adopt Eqs. (2) and (3) from Ref. [46], which express the BLR and DT energy densities as functions of the distance r between the emission region and the SMBH. Once $N_{\rm e}(\gamma_{\rm e})$ is obtained, we calculate the synchrotron, SSC, and EC emission from primary electrons using the public Python package `NAIMA`,[47] with synchrotron self-absorption (SSA) also taken into account.

2.2. Emission from Hadronuclear Interactions.

Here we consider the pp interactions between relativistic protons and cold protons within the jet. Relativistic protons are assumed to be injected with a power-law energy distribution at a constant rate, $\dot{Q}_{\rm p}^{\rm inj}(\gamma_{\rm p}) = \dot{Q}_{\rm p,0}\gamma_{\rm p}^{-p_{\rm p}}H(\gamma_{\rm p};\gamma_{\rm p,min},\gamma_{\rm p,max})$, where $\gamma_{\rm p,min/max}$ are the minimum and maximum proton Lorentz factors, $p_{\rm p}$ is the spectral index. Similarly, by giving a proton injection luminosity $L_{\rm p,inj}$, $\dot{Q}_{\rm p,0}$ can be obtained. By taking into account the cooling from pp interactions, the proton-synchrotron cooling, and the escape of the protons, the steady-state proton density distribution can be derived, which can be approximated as $N_{\rm p}(\gamma_{\rm p}) \approx \dot{Q}_{\rm p}^{\rm inj}(\gamma_{\rm p})\min\{t_{\rm pp}, t_{\rm dyn}, t_{\rm p,syn}\}$, with $t_{\rm p,syn} = \frac{6\pi m_{\rm e}c^2}{(c\sigma_{\rm T}B^2\gamma_{\rm p})(m_{\rm e}/m_{\rm p})^3}$ being the proton-synchrotron cooling timescale, and $t_{\rm pp} = \frac{1}{K_{\rm pp}\sigma_{\rm pp}n_{\rm H}c}$ being the cooling timescale of pp interactions, where $n_{\rm H}$ represents the number density of cold protons in the jet, $K_{\rm pp} \approx 0.5$ is the inelasticity coefficient, and $\sigma_{\rm pp}$ is the cross section for inelastic pp interactions.[48] More specifically, as suggested by Ref. [33], $n_{\rm H} = \frac{(1-\chi_{\rm p})\xi L_{\rm Edd}}{\pi R^2\Gamma^2 m_{\rm p}c^3}$, where $\chi_{\rm p}$ represents the ratio of the proton injection power to the total jet power,

and $\xi \leqslant 1$ is the ratio of the total jet power to the Eddington luminosity of the SMBH $L_{\rm Edd}$.

The *pp* interactions generate neutral and charged pions, which are short-lived and eventually decay into secondary particles, including γ-ray photons, electrons/positrons, and neutrinos, i.e.,

$$\begin{aligned} &p + p \to \pi^0 \to \gamma + \gamma, \\ &p + p \to \pi^+ \to \nu_\mu + \mu^+ \to \nu_\mu + e^+ + \nu_{\rm e} + \bar{\nu}_\mu, \\ &p + p \to \pi^- \to \bar{\nu}_\mu + \mu^- \to \bar{\nu}_\mu + e^- + \bar{\nu}_{\rm e} + \nu_\mu. \end{aligned}$$

With the steady-state $N_{\rm p}(\gamma_{\rm p})$, the differential spectrum of the secondary particles produced in unit time are calculated following the semianalytic method developed by Ref. [48]. The energy distribution of γ-ray induced pair cascades is evaluated using a semianalytical method developed in Ref. [10]. The leptonic emission of secondary pairs is calculated using `NAIMA` as well.

2.3. Parameter Constraints. In this one-zone hadronuclear model, there are nineteen parameters that describe the electrons, protons, and emitting region. Our strategy for further reducing the number of free parameters is described below.

1. Here we take the mass of Ap Librae's SMBH as $10^{8.4} M_\odot$.[49] Then the corresponding Eddington luminosity of the SMBH is $L_{\rm Edd} = 3.5 \times 10^{46}\,{\rm erg/s}$ and Schwarzschild radius of the SMBH is $R_{\rm S} \approx 7.4 \times 10^{13}\,{\rm cm}$.
2. Based on two basic conditions, namely that π^0 decay gamma rays in *pp* interactions contribute to the VHE spectrum and that the introduced total jet power does not exceed $L_{\rm Edd}$, our previous work[33] found that the radius of the emission region will be strictly constrained by
$$R \leqslant R_{\rm S} \frac{\sigma_{\rm pp}}{12\sigma_{\rm T}} \frac{\delta_{\rm D}^4}{\Gamma^4} \frac{L_{\rm Edd}}{L_{\rm TeV}^{\rm obs}} \approx 5.8 \times 10^{16}\,{\rm cm}, \quad (1)$$
where $\sigma_{\rm pp} = 6 \times 10^{-26}\,{\rm cm}^2$ is the cross section for inelastic *pp* interactions, $\sigma_{\rm T}$ is the Thomson scattering cross section, and $L_{\rm TeV}^{\rm obs} \approx 5.4 \times 10^{42}\,{\rm erg \cdot s^{-1}}$ is the VHE luminosity of Ap Librae.
3. As suggested by Ref. [33], we set $\chi_{\rm p} = 0.5$ to get the maximum parameter space. It indicates that the kinetic power of cold protons and the relativistic proton injection power each account for half of the total jet power. As shown in Ref. [33], adjusting the value of $\chi_{\rm p}$ slightly reduces the π^0-decay gamma-ray luminosity, but this effect can be compensated by tuning other parameters, such as ξ.
4. As studied by Ref. [33], since relativistic protons dominate the jet power, the proton injection power can be estimated as $L_{\rm p,inj} = \chi_{\rm p} \xi L_{\rm Edd}/\Gamma^2$.
5. The optical spectrum of Ap Librae is obtained during its faint state.[50] Here we set $L_{\rm BLR}^{\rm AGN} = 2.2 \times 10^{41}\,{\rm erg \cdot s^{-1}}$, as estimated by Ref. [51]. It should be noted that, as a BL Lac object, its spectral features are relatively weak, which may lead to fluctuations in the luminosity estimates of its emission lines. This primarily affects the determination of the characteristic locations of the BLR and DT when estimating their energy densities, thereby introducing some influence on the model fitting. Such effects can be mitigated by appropriately adjusting the position of the emission region r.
6. We adopt a typical value of $\gamma_{\rm e,min} = 100$ for simplicity, since its exact value cannot be constrained in a straightforward manner by the SED fitting because of the SSA effect.
7. As studied in Ref. [24], $\gamma_{\rm e,max} < 10^5$ is required to avoid overshooting the X-ray spectrum.
8. We adopt $\gamma_{\rm p,min} = 1$ for the minimum proton Lorentz factor. Its exact value will not affect our fitting results, but only the energetic requirements.
9. For simplicity, we set $p_{\rm p} = 2$ as a fiducial value.
10. Generally, $\gamma_{\rm p,max}$ can be obtained by equating the acceleration timescale to the minimum of the energy loss and escape timescales. The acceleration timescale can be evaluated by
$$t_{\rm acc} \simeq \frac{\alpha r_{\rm L}}{c} \simeq \frac{\alpha \gamma_{\rm p} m_{\rm p} c}{eB}, \quad (2)$$
where $r_{\rm L}$ is the Larmor radius of the relativistic proton and $\alpha \geqslant 1$ parameterizes the deviation from the largest possible particle acceleration rate (see Refs. [52] and [53] for fast and slow accelerations in simulation, respectively). Assuming that the acceleration is hindered by physical escape from the system, the maximum proton Lorentz factor is
$$\begin{aligned} \gamma_{\rm p,max} &= \frac{eBR}{\alpha m_{\rm p} c^2} \\ &\simeq 6.4 \times 10^7 \Big(\frac{\alpha}{50}\Big)^{-1} \Big(\frac{B}{1{\rm G}}\Big) \Big(\frac{R}{10^{16}\,{\rm cm}}\Big). \end{aligned} \quad (3)$$

Finally, nineteen free parameters are reduced to eleven, namely B, $\delta_{\rm D}$, $R \leqslant 5.8 \times 10^{16}\,{\rm cm}$, r, $L_{\rm e,inj}$, $p_{\rm e,1/2}$, $\gamma_{\rm e,b/max}$, $\alpha \geqslant 1$, $\xi \leqslant 1$.

3. Application. We apply the one-zone *pp* model described above to reproduce the multi-wavelength SED of Ap Librae. The fitting results are shown in Fig. 1, and the free and fixed/derived parameters are shown in Table 1. It can be seen that the SED from optical to GeV bands is mainly explained by the synchrotron, SSC, and EC emissions from primary electrons. However, due to the constraints imposed by the X-ray data on $\gamma_{\rm e,max}$ and $p_{\rm p,2}$, EC emission cannot provide a satisfactory explanation for the VHE spectrum, which is consistent with previous studies. In our modeling, the VHE data discovered by the HESS Collaboration[23] is interpreted by the γ-ray emission from π^0 decay in *pp* interactions. In Fig. 1, the sensitivity of CTA in the Southern Hemisphere is shown by the orange dot-dashed line. It can be seen that the γ-ray emission from π^0 decay not only accounts for the HESS observational data points, but its flat spectrum is expected to extend into higher-energy bands, beyond the detection sensitivity of CTA. If CTA in the future is able to detect the harder high-energy spectrum of Ap Librae,

Table 1. Parameters for SED fitting with the one-zone *pp* model.

Free parameters	B (G)	$\delta_{\rm D}$	R (cm)	r (pc)	$L_{\rm e,inj}$ (erg·s^{-1})	$p_{\rm e,1}$	$p_{\rm e,2}$	$\gamma_{\rm e,b}$	$\gamma_{\rm e,max}$	α	ξ	
Values	0.24	35	1.1×10^{15}	0.11	1.8×10^{41}	1.3	4	1.2×10^{3}	2.1×10^{4}	10^{3}	0.6	
Fixed/derived parameters	$L_{\rm BLR}^{\rm AGN}$ (erg·s^{-1})	$L_{\rm p,inj}$ (erg·s^{-1})	$\gamma_{\rm e,min}$	$\gamma_{\rm p,min}$	$\gamma_{\rm p,max}$	$p_{\rm p}$	$\chi_{\rm p}$	$U_{\rm H}$ (erg·cm^{-3})	$U_{\rm B}$ (erg·cm^{-3})	$U_{\rm e}$ (erg·cm^{-3})	$U_{\rm p}$ (erg·cm^{-3})	$f_{\rm pp}$
Values	2.2×10^{41}	8.5×10^{42}	100	1	6.6×10^{4}	2	0.5	3.6×10^{2}	2.3×10^{-3}	1.4	2.6×10^{2}	3.6×10^{-6}

Notes. The *pp* interaction efficiency $f_{\rm pp} = t_{\rm dyn}/t_{\rm pp}$ is obtained by setting a constant cross section for inelastic *pp* interactions $\sigma_{\rm pp} = 6\times10^{-26}\,{\rm cm}^2$.

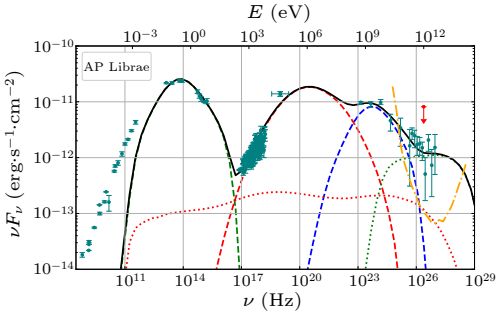

Fig. 1. Modeling result of the average-state multi-wavelength SED of Ap Librae core. The teal data points are taken from Ref. [28]. The VHE data points are the de-absorbed spectral points using the extragalactic background light model of Ref. [55]. Red data point is the 10-year upper limit of high-energy neutrinos with spectral index of 2 given by Ref. [54]. Orange dot-dashed curve shows the sensitivity of CTA in the southern sky.[56] The dashed green, red, and blue curves represent the synchrotron, SSC, and EC emissions from primary relativistic electrons, respectively. The dotted red curve represents the emission from pair cascades. The dotted green curve shows the γ-ray emission from π_0 decay in *pp* interaction. The solid black curve is the total emission from the emitting region.

this would suggest an origin in π^0 decay from *pp* interactions, since alternative radiation models predict only soft spectra.[12,24,28–30] By measuring the spectral index and the maximum energy of the photon spectrum, one can better constrain the shape of the proton spectrum, thereby providing deeper insights into the particle acceleration mechanisms within the jet. Please note that radio data below 10^{12} Hz are not explained here, as the SSA effect is unavoidable in a one-zone model. It would be more natural to interpret the radio data by synchrotron emission originating from the extended jet.[12] Following Ref. [54], we have included the 90% statistics-only upper limit for neutrino emission from AP Librae at 1 TeV (for a spectral index of -2.0) in Fig. 1 (red point with arrow). It can be seen that the π^0 decay spectrum, which resembles the neutrino spectrum, is much lower than the flux upper limit. This implies that introducing the *pp* interactions does not conflict with IceCube's non-detection conclusion regarding Ap Librae.

The model-predicted jet power carried by relativistic electron, cold proton, relativistic protons, magnetic field, and radiation can be derived through $P_{\rm jet} = \sum_i \pi R^2 \Gamma^2 c U_i$, where $U_i (i = {\rm e, H, p, B, r})$ are the energy densities associated with the emitting electron $U_{\rm e} = m_{\rm e}c^2 \int N_{\rm e}(\gamma_{\rm e})\gamma_{\rm e} d\gamma_{\rm e}$, cold proton $U_{\rm H} = m_{\rm p}c^2 n_{\rm H}$, relativistic protons $U_{\rm p} = m_{\rm p}c^2 \int N_{\rm p}(\gamma_{\rm p})\gamma_{\rm p} d\gamma_{\rm p}$, magnetic field $U_{\rm B} = B^2/8\pi$, and radiation $U_{\rm r} = \frac{L_{\rm obs}}{4\pi R^2 c \delta^4}$ with $L_{\rm obs}$ being the total non-thermal luminosity.[43] Our result suggests that $P_{\rm jet} \approx 1.8\times10^{46}\,{\rm erg\cdot s^{-1}}$, i.e., a sub-Eddington jet power is required in our one-zone *pp* model. Previous modeling studies that invoked hadronic processes, such as proton synchrotron radiation and photohadronic interactions, have found that introducing a super-Eddington jet power is unavoidable in order to account for the VHE emission of Ap Librae.[12,30] Compared with the jet power obtained in a recent leptonic model that included cold protons,[29] our result is 3.6 times larger. Such an increase is reasonable once both relativistic and cold protons are taken into account.

4. Discussion and Conclusion. In Ref. [30], the possibility was examined that proton synchrotron emission in the extended kpc jet could explain the VHE emission of Ap Librae, under the assumptions of a blob radius of 10^{22} cm, a magnetic field strength of 1 mG, and a bulk Lorentz factor of 3. They found that a jet power exceeding 100 times the Eddington luminosity is needed. Here we employ the analytical approach of Ref. [17] to explore the physical parameter space, aiming to further identify whether alternative parameter combinations allow proton synchrotron radiation to account for the VHE spectrum of Ap Librae without invoking extreme physical parameters. In the method given by Ref. [17], the parameter space is limited by three constraints, which are that the total jet power (dominated by the injection power of relativistic protons and the power carried in magnetic field) does not exceed the Eddington luminosity, that relativistic protons can be accelerated to the required maximum energy (Hillas condition[57]), and that the emitting region is transparent to VHE photons, respectively. We first explored the parameter space with $R = 10^{22}$ cm, as adopted in Ref. [30]. As shown in the upper panel of Fig. 2, a highly super-Eddington jet power is unavoidable; in particular, when $B = 1$ mG and $\Gamma = 3$, the resulting jet power is consistent with the numerical results of Ref. [30]. We then examined the parameter space for smaller R. The lower panel of Fig. 2 illustrates the case of $R = 10^{17}$ cm, where sub-Eddington jet powers can indeed be achieved. Unfortunately, however, in this case protons cannot be accelerated to energies sufficient to explain the VHE emission. We further searched the parameter space for radii ranging from 10^{14} to 10^{18}, but found no parameter combinations that simultaneously satisfy the Hillas condition and

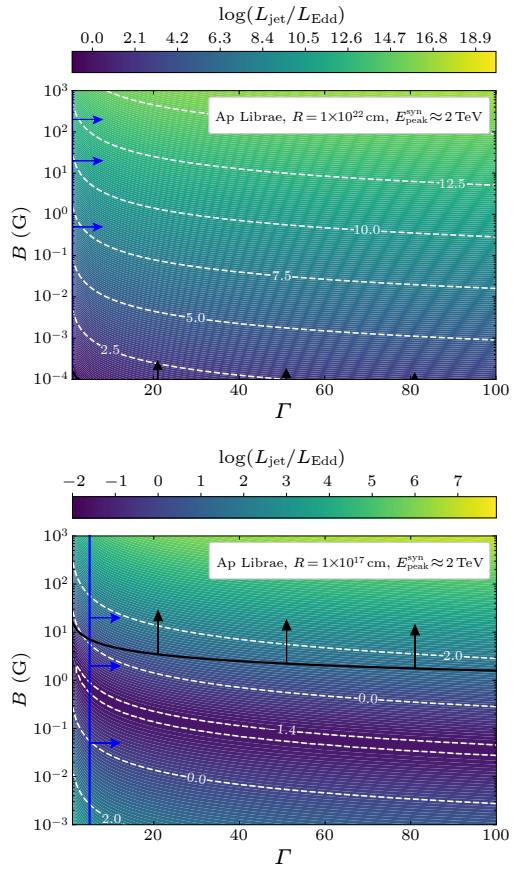

Fig. 2. The ratio of $L_{\rm jet}/L_{\rm Edd}$ in the Γ–B diagram for the one-zone proton-synchrotron model in the case of $R = 10^{22}$ cm (upper panel) and $R = 10^{17}$ cm (lower panel). The black curves with arrows represent the parameter space that satisfies the Hillas condition. The vertical blue curves with arrows show the lower limit of Γ that allows the escape of maximum energy γ-ray photons. The white dashed contours denote specific values of $\log(L_{\rm jet}/L_{\rm Edd})$ associated with the color bar.

the requirement of sub-Eddington jet power. In other words, proton synchrotron radiation cannot account for the VHE spectrum of Ap Librae without invoking extreme physical parameters.

It is worth noting that the value of R adopted in our model is very close to that used in Ref. [12], which primarily investigated photohadronic processes. One may therefore wonder whether the photohadronic processes not included in our model could be as significant as suggested by Ref. [12] in affecting the SED fitting. By comparing input parameters, it can be seen that $L_{\rm p,inj}$ and $\gamma_{\rm p,max}$ adopted in our model are about two orders of magnitude lower than those used in Ref. [12], so the efficiency of photohadronic interactions is significantly reduced. In addition, the lower $L_{\rm p,inj}$ further suppresses the flux generated by photohadronic processes. Considering the peak cross section of photomeson interactions due to the $\Delta^+(1232)$ resonance, the luminosity that can be produced by the highest-energy protons through photohadronic processes can be estimated through $f_{\rm p\gamma}\delta_{\rm D}^4 L_{\rm p,inj}/\ln\gamma_{\rm p,max}/(4\pi D_L^2) \approx 4\times10^{-16}\,{\rm erg\cdot s^{-1}\cdot cm^{-2}}$, where $D_{\rm L}$ represents the luminosity distance, $f_{\rm p\gamma}\approx10^{-28}\,{\rm cm^2}\,n_{\rm soft}(0.3\,{\rm GeV^2}/\gamma_{\rm p,max}m_{\rm p}c^2)R$ is the photomeson interaction efficiency with $10^{-28}\,{\rm cm^2}$ representing the photomeson cross section weighted by inelasticity, $n_{\rm soft}(0.3\,{\rm GeV^2}/\gamma_{\rm p,max}m_{\rm p}c^2)$ is the number density of target photons. It can be seen that the flux from photomeson interactions is far below the TeV emission of Ap Librae detected by HESS, which means that photohadronic contributions can be regarded as negligible in our model. In contrast to the photohadronic model adopted in Ref. [12], our *pp* model achieves the fit with sub-Eddington jet power, avoiding the need for extreme jet energetics.

In summary, our study demonstrates that the one-zone *pp* model can successfully reproduce the multiwavelength SED of Ap Librae, particularly its challenging TeV component, while requiring only sub-Eddington jet powers. This contrasts with previous proton-synchrotron or photohadronic models, which inevitably invoked extreme energetics. Although further observational constraints, especially from neutrino detections and future TeV observations, will be crucial to test the *pp* scenario, our results highlight that *pp* interactions provide a physically plausible and energetically economical pathway for explaining the VHE emission of Ap Librae. More broadly, this work suggests that *pp* processes may constitute an essential ingredient in the high-energy emission mechanisms of blazars, complementing leptonic and other hadronic channels.

Acknowledgements. We sincerely thank Michael Zacharias for sharing the SED data. This work was supported by the National Key R&D Program of China (Grant No. 2023YFB4503300), and the National Natural Science Foundation of China (Grant Nos. 12203043, 12263009, and 12203024).

References

[1] Urry C M and Padovani P 1995 *PASP* **107** 803
[2] Rani B 2019 *Galaxies* **7** 23
[3] Marscher A P and Gear W K 1985 *Astrophys. J.* **298** 114
[4] Maraschi L, Ghisellini G, and Celotti A 1992 *Astrophys. J. Lett.* **397** L5
[5] Dermer C D, Schlickeiser R, and Mastichiadis A 1992 *Astron. Astrophys.* **256** L27
[6] Dermer C D and Schlickeiser R 1993 *Astrophys. J.* **416** 458
[7] Aharonian F A 2000 *New Astron.* **5** 377
[8] Mücke A and Protheroe R J 2001 *Astropart. Phys.* **15** 121
[9] Aharonian F A 2002 *Mon. Not. R. Astron. Soc.* **332** 215
[10] Böttcher M, Reimer A, Sweeney K, and Prakash A 2013 *Astrophys. J.* **768** 54
[11] Cerruti M, Zech A, Boisson C, and Inoue S 2015 *Mon. Not. R. Astron. Soc.* **448** 910
[12] Petropoulou M, Vasilopoulos G, and Giannios D 2017 *Mon. Not. R. Astron. Soc.* **464** 2213
[13] Reimer A, Böttcher M, and Buson S 2019 *Astrophys. J.* **881** 46
[14] Das S, Gupta N, and Razzaque S 2020 *Astrophys. J.* **889** 149
[15] Das S, Razzaque S, and Gupta N 2022 *Astron. Astrophys.* **658** L6
[16] Xue R, Wang Z R, and Li W J 2022 *Phys. Rev. D* **10** 103021
[17] Xue R, Huang S T, Xiao H B, and Wang Z R 2023 *Phys. Rev. D* **107** 103019

[18] Wang Z R, Xue R, Xiong D, Wang H Q, Sun L M, Peng F K, and Mao J 2024 *Astrophys. J. Suppl.* **271** 10
[19] Ouyang Z, Xiao H, Manganaro M, Xie S, Wu J, Chen J, Xue R, Wang G, Zhang S, and Fan J 2025 *Astrophys. J.* **980** 19
[20] Xue R, Wang Z R, and Hu H B 2025 *Eur. Phys. J. C* **85** 779
[21] Xue R, He J C, Xiong D, and Wang Z R 2025 *Astrophys. J.* **990** 170
[22] Note1, the other TeV LBL is OT 081, whose TeV emission can be well explained by leptonic radiation. [58]
[23] Abramowski A, Aharonian F, Ait Benkhali F *et al.* 2015 *Astron. Astrophys.* **573** A31
[24] Sanchez D A, Giebels B, Fortin P *et al.* 2015 *Mon. Not. R. Astron. Soc.* **454** 3229
[25] Kaufmann S, Wagner S J, and Tibolla O 2013 *Astrophys. J.* **776** 68
[26] Tavecchio F, Ghisellini G, Ghirlanda G, Foschini L, and Maraschi L 2010 *Mon. Not. R. Astron. Soc.* **401** 1570
[27] Hervet O, Boisson C, and Sol H 2015 *Astron. Astrophys.* **578** A69
[28] Zacharias M and Wagner S J 2016 *Astron. Astrophys.* **588** A110
[29] Roychowdhury A, Meyer E T, Georganopoulos M, Breiding P, and Petropoulou M 2022 *Astrophys. J.* **924** 57
[30] Pratim Basumallick P and Gupta N 2017 *Astrophys. J.* **844** 58
[31] Banik P and Bhadra A 2019 *Phys. Rev. D* **99** 103006
[32] Banik P, Bhadra A, Pandey M, and Majumdar D 2020 *Phys. Rev. D* **101** 063024
[33] Li W J, Xue R, Long G B, Wang Z R, Nagataki S, Yan D H, and Wang J C 2022 *Astron. Astrophys.* **659** A184
[34] Mondal S K, Das S, and Gupta N 2023 *Astrophys. J.* **948** 75
[35] Majumdar J, Maurya S, and Prince R 2025 *J. High Energy Astrophys.* **48** 100402
[36] Bennett C L, Larson D, Weiland J L, and Hinshaw G 2014 *Astrophys. J.* **794** 135
[37] Ghisellini G, Tavecchio F, Maraschi L, Celotti A, and Sbarrato T 2014 *Nature* **515** 376
[38] Madejski G M, Nalewajko K, Madsen K K *et al.* 2016 *Astrophys. J.* **831** 142
[39] Tan C, Xue R, Du L M, Xi S Q, Wang Z R, and Xie Z H 2020 *Astrophys. J. Suppl.* **248** 27
[40] Zech A and Lemoine M 2021 *Astron. Astrophys.* **654** A96
[41] Zdziarski A A, Phuravhathu D G, Sikora M, Böttcher M, and Chibueze J O 2022 *Astrophys. J. Lett.* **928** L9
[42] Note2, in different reference frames, certain parameters will vary. Taking frequency ν as an example, we have $\nu = (1+z)\nu^{\rm obs}/\delta_{\rm D} = \nu^{\rm AGN}/\delta_{\rm D}$. For the transformation of other parameters across reference frames, one may refer to several classic textbooks on high-energy astrophysics (e.g., see Ref. [59]).
[43] Ghisellini G, Tavecchio F, Foschini L, Ghirlanda G, Maraschi L, and Celotti A 2010 *Mon. Not. R. Astron. Soc.* **402** 497
[44] Schlickeiser R and Ruppel J 2010 *New J. Phys.* **12** 033044
[45] Hu H B, Wang H Q, Xue R, Peng F K, and Wang Z R 2024 *Mon. Not. R. Astron. Soc.* **528** 7587
[46] Hayashida M, Madejski G M, Nalewajko K *et al.* 2012 *Astrophys. J.* **754** 114
[47] Zabalza V 2015 *34th International Cosmic Ray Conference* (ICRC2015) p. 922
[48] Kelner S R, Aharonian F A, and Bugayov V V 2006 *Phys. Rev. D* **74** 034018
[49] Woo J H, Urry C M, van der Marel R P, Lira P, and Maza J 2005 *Astrophys. J.* **631** 762
[50] Morris S L and Ward M J 1988 *Mon. Not. R. Astron. Soc.* **230** 639
[51] Stickel M, Fried J W, and Kuehr H 1993 *Astron. Astrophys.* **98** 393
[52] Zhang H, Sironi L, Giannios D, and Petropoulou M 2023 *Astrophys. J. Lett.* **956** L36
[53] Petropoulou M, Psarras F, and Giannios D 2023 *Mon. Not. R. Astron. Soc.* **518** 2719
[54] Abbasi R, Ackermann M, Adams J *et al.* 2025 arXiv:2501.16440 [astro-ph.HE]
[55] Franceschini A, Rodighiero G, and Vaccari M 2008 *Astron. Astrophys.* **487** 837
[56] Actis M, Agnetta G, Aharonian F *et al.* 2011 *Exp. Astron.* **32** 193
[57] Hillas A M 1984 *Annu. Rev. Astron. Astrophys.* **22** 425
[58] Abe H, Abe S, Acciari V A *et al.* 2025 *Mon. Not. R. Astron. Soc.* **540** 364
[59] Ghisellini G 2013 *Radiative Processes in High Energy Astrophysics* (Springer Cham) **873**